Journal of Ceramic Processing Research. Vol. 17, No. 10, pp. 1063~1067 (2016)

J O U R N A L O F
Ceramic Processing Research

Mineral phase, microstructure, and Infra-Red characteristics of calcia-stabilized zirconia nanocrystallines synthesized from local zircon and slaked lime

Dede Taufik[a], Mikrajuddin Abdullah[b], Hernawan[a], Suhanda Sutardi[a] and Rifki Septawendar[a,c,*]

[a]*Division of Research and Standardization, Center for Ceramics, Ministry of Industry of Indonesia, Akhmad Yani 392, Bandung 40272, West Java, Indonesia*

[b]*Department of Physics, Institut Teknologi Bandung, Ganesa 10, Bandung, West Java, Indonesia*

[c]*Laboratory of Advanced Material Processing, Department of Engineering Physics, Institut Teknologi Bandung, Ganesa 10, Bandung, West Java, Indonesia*

Nanocrystallines of calcia-stabilized zirconia are known to reveal excellent mechanical and high ionic conductivity properties whose depend on the calcia concentration. In this work, nanocrystallines of calcia-stabilized zirconia were synthesized from zircon precursor and 7.5 weight % CaO at 1000 ºC, 1200 ºC, and 1400 ºC. Phase transformation and microstructure evolution were investigated by an X-ray diffraction and a scanning electron microscopy. Another un-doped zirconia was also synthesized from the local zircon by following the same procedure for comparison. A fully cubic form of the calcia-stabilized zirconia and calcium zirconate were obtained at 1200°C having the crystallite sizes ranging from 55 to 87 nm and remained stable at 1400 ºC. Meanwhile, un-doped zirconia consisted of pure the monoclinic zirconia at 1200 ºC and 1400 ºC. High agglomeration is found in the calcia-stabilized zirconia particles at 1000 ºC, whereas grain boundaries and interconnect are observed at 1400 ºC. The cubic crystal of zirconia has specific and different finger print characteristics in the infra-red spectrum compared to the monoclinic zirconia.

Key words: 7.5 wt% calcia-stabilized zirconia, Zircon, Slaked lime, Phase alteration and Microstructure evolution.

Introduction

Zirconia is a promising material and frequently used in many conventional and advanced applications such as nozzles, refractories, dental materials, fuel cells, and catalysts. Nevertheless, pure zirconia exhibits some improper properties, low mechanical properties and a low ionic conductivity, for instance [1, 2]. Therefore, some lower-valence metal oxides are added to stabilize zirconia in order to enhance its properties [3-5]. For example, calcia is often used as a dopant in zirconia to get the tetragonal or the cubic structures [5, 6]. These zirconia structures have different main properties; the tetragonal zirconia exhibits excellent mechanical properties [5], whereas the cubic zirconia shows high ionic conductivity at high temperatures [7, 8]. The phase composition of calcia-stabilized zirconia depends on the calcia concentration as the dopant [9, 10].

A number of techniques have been reported on the preparation of microcrystalline and nanocrystalline calcia-stabilized zirconia (CSZ) powders, such as solid state reaction [4, 10], a coprecipitation method [11], a polymeric precursor route [11, 12], a sol-gel method [13], hydrothermal processing [14], a solution combustion method [15], milling process [5] and calcination masking gel [6]. Most of these techniques on calcia-stabilized zirconia synthesis used organometallic compounds and salts as the zirconium precursors, which were less economic than zircon precursor. Some works on preparation of stabilized zirconia from zircon precursor were successfully conducted, as reported by Manivasakan et al. [16] and El-Tawill, et al. [17]. Manivasakan, et al. [16], "synthesized sodium stabilized cubic zirconia from raw zircon sand using a chemical extraction process followed by a ball mill-aided precipitation route". El-Tawill, et al. [17], "successfully prepared cubic zirconia from zircon sand by firing with CaO/MgO mixture at 1500 ºC and after separating the silica by acid leaching". The last technique is the most relevant on synthesis of CSZ but it takes a lot of costs because of high energy consumption.

In this work, nanocrystallines of the cubic stabilized zirconia was synthesized from zircon precursor with calcia as a dopant. Duwez, et al. [18] reported that the amount of calcia required to stabilize zirconia in the fluorite-type cubic phase was between 8 and 17 weight % at various temperatures between 815 ºC and 1375 ºC [18]. This result seems to be different from the findings of Stubican and Pray [19]. Stubican and Pray [19] found crystallization of the fluorite-type cubic phase of zirconia at a lower concentration of calcia of about 7.5 weight % at 850 ºC and the calcia-stabilized zirconia

*Corresponding author:
Tel : +62-857-5999-7747
Fax: +6222-720-5322
E-mail: rifkiseptawendar@gmail.com

remains cubic at temperatures 1000 °C-2000 °C. Therefore, about 7.5 weight % CaO was used as a stabilizer on the synthesis of CSZ nanocrystallines in this work. However, this work reports a simple method on synthesis of nanocrystalline CSZ using inexpensive local precursors at relative low-temperature calcination. Nanocrystallines of CSZ was synthesized from local zircon precursor and local slaked lime ($Ca(OH)_2$) through wet milling process. The as-synthesized CSZ was calcined at elevated temperatures from 1000 °C to 1400 °C. The objectives of this work are to synthesize nanocrystallines CSZ from local precursors through wet milling process, to study its phase transformation and microstructure evolution during thermal treatment with X-ray diffraction (XRD) and scanning electron microscopy (SEM) studies, and to distinguish characteristics of CSZ's infra-red spectrum compared to un-doped zirconia.

Experimental Procedure

Materials and instruments

Local zircon ($ZrSiO_4$) was obtained from PT. Monokem Surya Indonesia consisting of 64.51% of ZrO_2, 31.31% of SiO_2, and 0.95% of HfO_2 as major components, and the beneficiated Indonesian origin limestone was obtained from Padalarang-West Java, Indonesia. The other material utilized in this work were sodium carbonate (Na_2CO_3), a 96% sulfuric acid solution, sodium hydroxide (NaOH), an ammonia solution, and carboxyl methyl cellulose (CMC) from the Indonesian local chemical distributor. The laboratory apparatus used were an alumina mill with 5 kg capacity, a hydraulic press, a gas furnace with the maximum temperature of 1300 °C, and an electric furnace with the maximum temperature of 1500 °C. The analytical instruments used in this work were a Shimadzu Lab-X XRD-6000 X-ray diffractometer (XRD), ZEISS and JEOL JSM-35C scanning electron microscopes (SEMs), and a Shimadzu Fourier Transform Infra-Red (FT IR) Prestige 21 spectrometer.

Table 1. Chemical composition of $Zr(OH)_4$.

Oxides	$ZrO_2 + HfO_2$	SiO_2	SO_3	CaO	Fe_2O_3	Co_2O_3	ZnO
Percent (%)	90.761	4.410	4.304	0.299	0.200	0.014	0.012
Std.	0.105	0.054	0.031	0.002	0.004	0.003	0.001

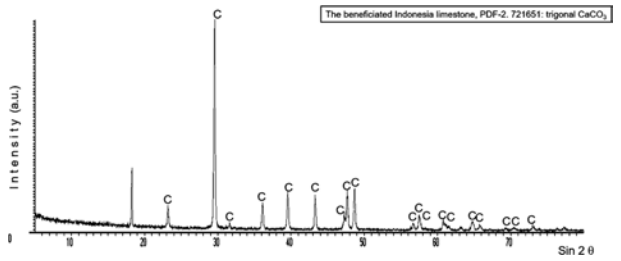

Fig. 1. The beneficiated Indonesian limestone.

Synthesis of 7.5 weight % Calcia-stabilized zirconia

Zirconium precursors, zirconium hydroxides, were extracted from local zircon through a low cost, facile method of sodium carbonate sintering [20]. Chemical compositions of zirconium hydroxide at 150 °C by an energy dispersive X-ray (EDX) spectroscopy are shown in Table 1. A starting material of calcium oxide was prepared from the calcined Indonesian limestone. An XRD pattern of the beneficiated Indonesian limestone from Padalarang-West Java is presented in Fig. 1.

The synthesis of CSZ was initially carried out by dissolving the zirconium hydroxide precursors in the acid solution until the final pH 4. Single component of calcia was prepared from limestone. The local limestone was initially calcined at 900 °C to produce lime. The amount of lime weighed had to produce 7.5 weight % CaO of zirconia. The appropriate amount of lime was blended with water to give "slaked lime", calcium hydroxides ($Ca(OH)_2$). The slaked lime was then mixed with the zirconia precursors in an alumina pot mill, then pH of the mixture was adjusted by adding an ammonia solution to the mixture until neutral condition under vigorous milling for 8 hrs. The as-synthesized CSZ was then dried in an oven at approximately 100 °C and was continuously calcined at 1000 °C, 1200 °C, and 1400 °C for 1 hr. Another batch of un-doped zirconia was also prepared from the local zircon by following the same procedure for comparison of the zirconia phase transformation and infra-red spectra. However, the calcination temperature of this un-doped zirconia was only applied at 1200 °C and 1400 °C for 1 hr.

Characterization

Crystalline phases of CSZ and und-doped zirconia were identified by an XRD instrument using Shimadzu Lab-X XRD-6000 X-ray diffractometer at 40 Kv and 30 mA with Cu/Kα (λ = 1.54060 Å) radiation source. The diffraction patterns were scanned from 10.0150 to 79.9750 and 90.0800 (2θ) with angular step of 0.0200-0.0300. Crystallite sizes were estimated from XRD peak widths using the Scherrer equation [1].

$$D = \frac{K\lambda}{\beta \cos\theta} \quad (1)$$

where D is the crystallite size, K is a shape factor with a value of 0.9-1.4, λ is the wavelength of the X-rays (1.540598 Å), θ is Bragg's angle and β is the full width at half maximum (FWHM). XRD patterns were identified using the PDF2, JCPDS-International Centre for Diffraction Data.

SEM analysis was carried out to observe microstructure evolution of the calcined CSZ at elevated temperatures using ZEISS and JEOL JSM-35C SEMs. A Shimadzu FT-IR Prestige 21 spectrometer was used to analysis infra-red spectra of CSZ and un-doped zirconia.

Results and Discussion

Phase transformation of CSZ at elevated temperatures

The powder XRD analysis results of which are shown in Fig. 2, shows the phase transformations of CSZ at elevated temperatures of 1000 ºC, 1200 ºC, and 1400 ºC. Based on Fig. 2, the as-synthesized CSZ from zirconium hydroxide and slaked lime starting materials consisted of the monoclinic and the cubic phases of zirconia at 1000 ºC. The main peaks of the m-ZrO_2 appear at diffraction angles 2θ of 28.23 º and 31.55 º, corresponding to the ($\bar{1}11$) and (111) crystal planes of the m-ZrO_2 structure, respectively (PDF-2. 830944). Meanwhile, the peaks of the c-ZrO_2 are identified at diffraction angles 2θ of 30.16 º, 34.94 º, 50.21 º, 59.67 º, 62.57 º, and 73.70 º, corresponding to the (111), (200), (220), (311), (222), and (400) crystal planes of the c-ZrO_2 structure, respectively, as according to PDF-2. 811550 and PDF-2. 750359. The result is different from the finding of Septawendar, et al. [6]. They reported low-temperature crystallization at 800 ºC of the pure fluorite-type cubic phase of CSZ using salts as CSZ precursors. In addition, Septawendar et al. [16] used higher concentration of calcia than that used in our work, it was about 17 weight % calcia of zirconia. In a case, the type of CSZ starting or precursor materials and calcia concentration in the synthesis conditions perhaps controlled that emergence of different zirconia phases and crystallization temperature on CSZ. However, according to the powder XRD analysis results at 1000 ºC of which are shown in Fig. 1, calcia stabilizer started partially to penetrate the zirconia lattices and reacted with the metathetically formed ZrO_2 to result in a cubic solid solution [6]. It is strongly evidenced by the existence of the c- and the m-ZrO_2 phases in CSZ sample.

Nevertheless, by increasing temperature from 1000 ºC to 1200 ºC, the c-ZrO_2 peaks increased and the main peaks of the m-ZrO_2 significantly disappeared at diffraction angles 2θ of 28.23 º and 31.55 º, corresponding to the ($\bar{1}11$) and (111) crystal planes of the m-ZrO_2 structure (see in Fig. 2). At the moment, this phenomenon was also accompanied by the appearance of calcium zirconate ($CaZrO_3$) peaks at diffraction angles 2θ of 31.64 º and 22.31 º, corresponding to the (121) and (101)/(020) crystal planes of the orthorhombic $CaZrO_3$ structure, respectively (PDF-2. 350790 and PDF-2. 762401). After heating the as-synthesized CSZ at a higher temperature of 1400 ºC, the CSZ phases remains stable, consisting of the c-ZrO_2 and the o-$CaZrO_3$ phases. The phenomena on the CSZ phases at 1000 ºC, 1200 ºC and 1400 ºC is totally different from the report of Stubican and Pray [19]. Based on their finding, zirconia that stabilized with 7.5 weight % calcia should be only consisted of the cubic solid solution phase at those temperatures. Stubican and Pray [19] used powder zirconium oxide and calcined calcium carbonate in their experiment, whereas zirconium hydroxide and calcium hydroxide were used as CSZ starting materials in this work. Thus, the appearance of different phases due to the specific conditions of the synthesis process, such as the type of starting materials, medium, and mixing process during preparation. The direct phase transformation of the as-synthesized CSZ during thermal treatment at elevated temperatures could be assumed as follows:

$$\text{as-synthesized CSZ} \xrightarrow{1000\ ^{o}C} \text{m-}ZrO_2 + \text{c-}ZrO_2(CaO) \quad (2)$$

$$\text{m-}ZrO_2 + \text{c-}ZrO_2(CaO) \xrightarrow{1400\ ^{o}C} \text{c-}ZrO_2(CaO) + CaZrO_3 \quad (3)$$

Since calcia used as a dopant in 7.5 weight % of zirconia, the fluorite-type cubic phase of zirconia was obtained at 1200 ºC and 1400 ºC along with $CaZrO_3$ as a minor component. However, un-doped zirconia that synthesized from local zircon consists of a single phase of the monoclinic zirconia at 1200 ºC and it remains stable after heating at 1400 ºC, as shown by the powder XRD analysis results in Fig. 3. Therefore, it can be figured out that the CaO dopant has an important role on the stabilization of the fluorite-type cubic phase of zirconia.

Stabilization mechanism of the cubic solid solution ZrO_2 with CaO occurs through precise replacement of Ca^{2+} cations to Zr^{4+} cations in the crystal lattice of zirconia, resulting in one oxygen vacancy because of the charge compensation in zirconia lattice. Using

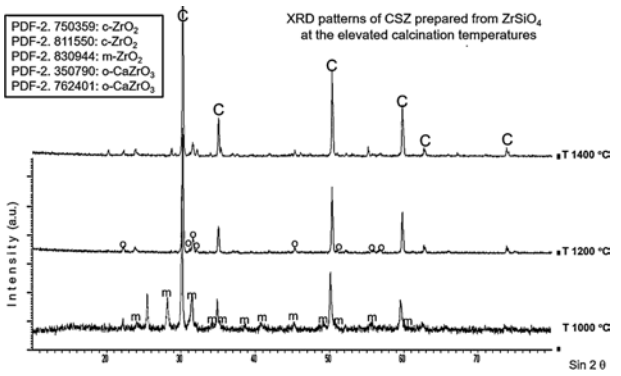

Fig. 2. XRD patterns of the as-synthesized CSZ at elevated calcination temperatures.

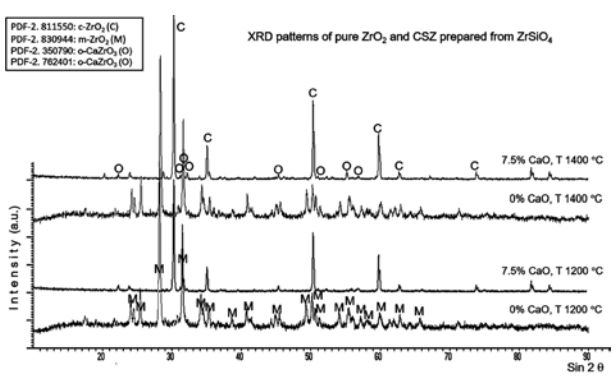

Fig. 3. XRD patterns of CSZ and un-dope zirconia at elevated temperatures.

Table 2. Quantitative results from the Scherrer method on the zirconia phases in CSZ at 1000 ° and 1200 °C.

Zirconia phase	Average crystallite size (nm)				Phase composition (%)	
	1000 °C		1200 °C		1000 °C	1200 °C
(hkl)	(111)	(222)	(111)	(222)		
c-ZrO_2 PDF2-811550 PDF2-750359	55	49	55	87	68.7	60.3
(hkl)	($\bar{1}$11)	(111)	($\bar{1}$11)	(111)		
m-ZrO_2 PDF2-830944	34	30	–	–	31.3	–
(hkl)	(121)	(101)/ (020)	(121)	(101)/ (020)		
o-$CaZrO_3$ PDF2-811550 PDF2-750359	–	–	40	36	–	39.7

Kroger-Vink notation [1], the stabilization mechanism of zirconia by calcia dopant can be created as follows:

$$CaO \xrightarrow{ZrO_2} Ca''_{Zr} + V''_O + O_o^x \quad (4)$$

Table 2 presents the powder XRD quantitative analysis results on the CSZ particles at 1000 °C and 1200 °C, by ignoring an unidentified phase. The Scherrer method was apply to calculate the crystallite sizes of the certain crystal planes of ZrO_2 and $CaZrO_3$ phases at 1000 °C and 1200 °C, based on the main peaks of the XRD patterns from Fig. 2, and assisted by using an XRD software. Table 2 shows that the average crystallite sizes of ZrO_2 and $CaZrO_3$ are less than 100 nm at the different elevated calcination temperatures.

Microstructure investigation of CSZ particles after thermal treatment

Nanocrystallines of CSZ particles were characterized by SEM after thermal treatment at elevated temperatures. Typical SEM images of the calcined CSZ nanocrystallines are displayed in Fig. 4. Typical SEM images in the left top and right top sides of Fig. 4, show microstructure of the as-synthesized CSZ that was calcined to 1000 °C. It is clearly seen that fine and uniform CSZ particles with high agglomeration were successfully synthesized from local precursors, having an average grain size below 200 nm. As the calcination temperature increased to 1200 °C, grain growth obviously occurs on CSZ sample (the left bottom side in Fig. 4). Calcia-stabilized zirconia grains with sizes closed to 1 μm were observed connecting against each other. When the calcination temperature was raised from 1200 °C to 1400 °C, the CSZ's microstructure evolution was clearly visible. Further grain growth took

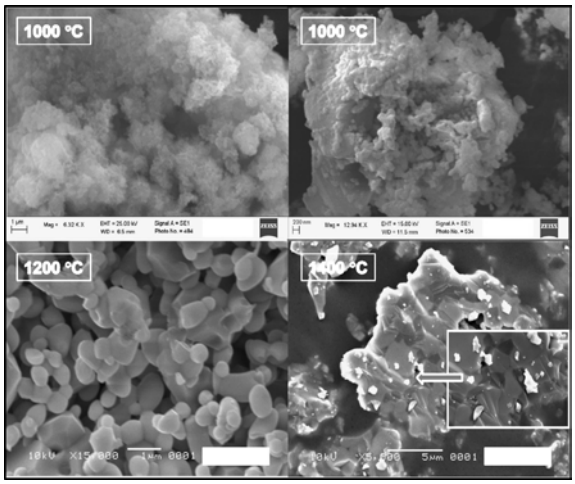

Fig. 4. Typical SEM images of the calcined CSZ nanocrystallines.

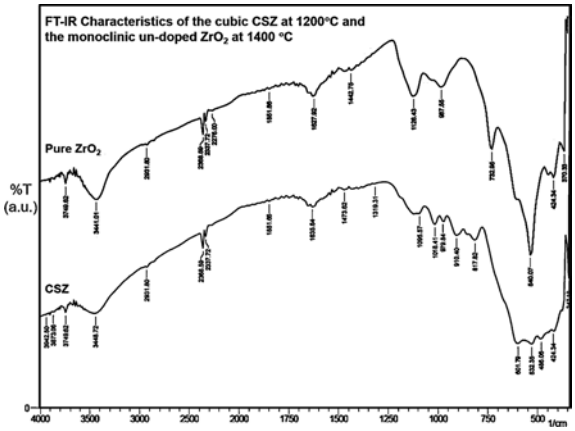

Fig. 5. FT-IR analysis results of CSZ and un-doped ZrO_2.

place; grain boundary, interconnect, and necking among the grain boundaries were found in CSZ sample. At a high temperature of 1400 °C, it is believed that surface diffusion and grain boundaries diffusion occurs much faster, as shown in Fig. 4 (a SEM image on the right bottom side).

Fourier Transform Infra-Red analysis of CSZ and un-doped ZrO_2

The FT-IR spectra of CSZ and un-doped ZrO_2 are presented in Fig. 5, shows the FT-IR spectra in the range from 4000 cm^{-1} to 340 cm^{-1}. The FT-IR spectrum of CSZ at 1200 °C shows specific finger print characteristics of the strong broad bands at 424.34 cm^{-1} ~ 601.79 cm^{-1} correspond to the cubic phase characteristics of the Zr-O bond vibrations [21]. The absorption peak of $CaZrO_3$ is particularly situated in 532.32 cm^{-1} that overlap with the Zr-O vibration band [13]. Meanwhile, CaO has weak absorption bands at 424.34 cm^{-1} which overlap with the Zr–O vibration band [22, 23], and 817.82 ~ 850.00 cm^{-1} [24].

The FT-IR spectrum of the un-doped zirconia synthesized from local zircon at 1400 °C is displayed in Fig. 5. The various vibrations of the Zr-O bond related

to monoclinic zirconia molecules they are noted in finger prints of 424.34 cm^{-1}, 540.07 cm^{-1} and 732.95 cm^{-1}. The bond of metal, oxygen, and metal (-Zr-O-Zr-) corresponding to the monoclinic zirconia structure it is observed at 540.07 cm^{-1}. The strong sharp bands at 540.07 cm^{-1} and 732.95 cm^{-1} arise from "internal vibrations of the monoclinic zirconia in the unit cell" [25].

According to the powder FT-IR analysis of CSZ and un-doped ZrO_2 in Fig. 5, it is obviously shown that the significant difference between FT-IR spectra of the cubic and the monoclinic zirconia is on their finger print characteristics of the absorption bands.

Conclusions

Nanocrystallines of CSZ were successfully synthesized from local zircon precursor and slaked lime via wet milling process and calcined at elevated temperatures. Nanocrystallines of CSZ have a fully cubic structure at 1200°C exhibiting the crystallite sizes ranging from 55 to 87 nm and remain stable at 1400 ºC. The powder microstructure analysis of CSZ show high agglomeration at 1000 ºC, whereas grain boundary, interconnect, and necking among the grain boundaries are observed at 1400 ºC. The cubic solid solution of calcia-stabilized zirconia show specific finger print characteristics of the strong broad bands at 424.34 cm^{-1} ~ 601.79 cm^{-1}.

Acknowledgments

The authors would like to acknowledge a good environment and facilities to complete this research by Center for Ceramics, Ministry of Industry of Indonesia. The authors would like to take this opportunity to thank to the Department of Physics Institut Teknologi Bandung for financial support. Also, the authors also thankful to PT. Vanadia Utama for SEM analysis (ZEISS SEM).

References

1. R. Septawendar, S. Suhanda and B.S. Purwasasmita, Journal of Ceramic Processing Research 16[4] (2015) 438-444.
2. N.Q. Minh, J. Am. Ceram. Soc. 76[3] (1993) 563-588.
3. R. Septawendar, B.S. Purwasasmita, and S. Suhanda, Journal of the Indonesian Ceramics and Glass 21[1] (2012) 44-59.
4. S. Serena, A. Caballero, and M.A. Sainz, Journal of the European Ceramic Society 33 (2013) 1413-1424.
5. A.O. Zhigachev, A.V. Umrikhin, Y.I. Golovin, and B.Y. Faber, Int. J. Appl. Ceram. Technol. 12[S3] (2015) E82-E89.
6. R. Septawendar, B.S. Purwasasmita, and S. Sutardi, Journal of the Australian Ceramic Society 49[1] (2013) 101-108.
7. R. Septawendar, B. Yuniarto, S. Suhanda, and B.S. Purwasasmita, A Review on Journal of the Indonesian Ceramics and Glass 23[2] (2014) 76-93.
8. Raghvendra and P. Singh, Journal of the European Ceramic Society 35[5] (2015) 1485-1493.
9. Y.-L. Huang, Y.-C. Lee, D.-C. Tsai, R.-H. Huang, and F.-S. Shieu, Ceramics International 40[1B] (2014) 2373-2379.
10. W.I. Emam, A.F. Mabied, H.M. Hashem, M.M. Selim, A.M. El-Shabiny, and I.S.A. Farag, Journal of Solid State Chemistry 228 (2015) 153-159.
11. R. Muccillo, R.C. Buissa Netto, and E.N.S. Muccillo, Matter. Lett. 49 (2001) 197-201.
12. K.R. Mohamed and E. El-Meliegy, Ceramics International 34 (2008) 285-292.
13. B. Liu, X. Lin, L. Zhun, X. Wang, and D. Xun, Ceramics International 40[8A] (2014) 12525-12531.
14. A. Rizzuti, A. Corradi, C. Leonelli, R. Rosa, R. Pielaszek, and W. Lojkowski, J. Nanopart. Res. 12 (2010) 327-335.
15. K. Boobalan, A.Varun, R.Vijayaraghavan, K. Chidambaram, and U.K. Mudali, Ceramics International 40 (2014) 5781-5786.
16. P. Manivasakan, V. Rajendran, P.R. Rauta, B.B. Sahu, and B.K. Panda, J. Am. Ceram. Soc. 94[5] (2011) 1410-1420.
17. S.Z. El-Tawil, K.A. El-Barawy, and A.A. Francis, Journal of the Ceramic Society of Japan 107[3] (1999) 193-198.
18. P. Duwez, F. Odell, and F. H. Brown, J. Am. Ceram. Soc. 35[5] (1952) 107-113.
19. V.S. Stubican and S.P. Ray, J. Am. Ceram. Soc. 60[11-12] (1977) 534-537.
20. R. Septawendar, S. Sutardi, U. Karsono, and N. Sofiyaningsih, Journal of the Australian Ceramic Society 42[2] (2016) 92-102.
21. N. Tiwari and V. Dubey, Journal of Biological and Chemical Luminescence 31[3] (2015) 837-842.
22. L. Berzina-Cimdina and N. Borodajenko, in "Research of Calcium Phosphates Using Fourier Transform Infrared Spectroscopy, Infrared Spectroscopy-Materials Science, Engineering and Technology" (InTech Press, 2012) p. 136-137.
23. A. Imtiaz, M.A. Farrukh, M. Khaleeq-ur-rahman, and R. Adnan, The Scientific World Journal 2013 (2013) 11 pages. http://dx.doi.org/10.1155/2013/641420.
24. W. Guan, F. Ji, Y. Cheng, Z. Fang, D. Fang, P. Yan, and Q. Chen, Journal of Nanomaterials 2013 (2013) 7.
25. R. Septawendar, S. Sutardi, B.S. Purwasasmita, and F. Edwin, Journal of the Australian Ceramic Society 48[1] (2012) 12-20.